JOURNAL OF SPACECRAFT AND ROCKETS
Vol. 47, No. 5, September–October 2010

Engineering Notes

Experimental and Numerical Simulation Study of Liquid-Propellant Draining from Rocket Tanks

Kiyoshi Kinefuchi,* Toru Kamita,† and Hideyo Negishi‡
Japan Aerospace Exploration Agency, Tsukuba 305-8505, Japan
and
Keisuke Yamada§ and Masanobu Fujimura¶
IHI Aerospace Company, Ltd., Tomioka 370-2398, Japan

DOI: 10.2514/1.48398

Nomenclature

a = vertical acceleration, m/s^2
Fr = Froude number
h = liquid height from baffle at center of tank, m
h_c = critical height, m
h_0 = liquid height from baffle at surface dip, m
Q = drain volume flow rate, m^3/s
r = drain line radius, m
R_b = baffle radius, m
u = liquid radial velocity at surface dip, m/s
v = liquid velocity in drain line, m/s
V_f = liquid volume at fixed point in tank, m^3
V_r = liquid volume remaining in tank at gas ingestion, m^3
δ = width of control volume, m
ρ = liquid density, kg/m^3

I. Introduction

AN UNDERSTANDING of the process by which liquid propellant drains from a rocket tank is important for propellant management, because residual propellant in the tank affects launch capability. Turbopump rocket engines must cut off before the pressurant gas enters the pump by means of gas ingestion or gas blow-through to prevent overrotation and possible critical launch failure. Thus, some amount of propellant always remains in the tank.

Several types of propellant management devices can be placed near the tank outlet; the configuration of the devices depends upon launch system requirements [1–4]. To better understand how to design these devices, we need to study the propellant-draining process. However, for such studies, large-scale or inflexible devices, such as full-scale propellant tanks with cryogenic propellant under high-acceleration or low-gravity conditions, are clearly impractical. Numerical procedures based on findings from small-scale experiments are much more desirable. Recently, with progress in computer technology and simulation techniques, a few numerical investigations have been performed [2]. However, few studies have reported 1) numerical simulations for the most common circular-plate-type device, 2) numerical methodologies, such as treatment of boundary layers and three-dimensional (3-D) effects, and 3) detailed flowfield investigations on dip formation and bubble behavior by comparing numerical simulations with the theoretical liquid remaining.

In this study, we investigated the draining process for the circular-plate-type device, using both experiments and numerical simulations in order to discover a potentially effective draining theory and carry out simulations for applications to actual rocket flights in the future. We used a small-scale tank and analyzed two-dimensional (2-D) and 3-D two-phase flows for both laminar and turbulent flows by comparing the results with a theoretical model based on Bernoulli's law. This paper presents a comparison of the experimental, numerical, and theoretical liquid remaining. The characteristics of the draining flow and the effectiveness of the theory and simulation are discussed in terms of the numerical simulation methodology.

II. Theoretical Model

Propellant tanks of launch vehicles generally contain a baffle: that is, a circular plate installed horizontally above the tank outlet [3]. Without a baffle, the liquid flow generates a large vortex, and pressurant gases readily enter the feed line [5,6]. The baffle delays gas ingestion into the turbopump.

Figure 1 shows a schematic of liquid draining from a rocket tank immediately before gas ingestion. The dip on the liquid's surface near the baffle edge appears and then grows rapidly. Finally, gas reaches the drain line connected to the rocket engine. We require an expression for the critical height of the liquid h_c, defined as the height of the liquid's surface measured from the baffle surface at the time the dip forms [7,8]. Bernoulli's law, applied between the bottom of the dip and the center of the surface, gives

$$\rho a h = \rho a h_0 + \tfrac{1}{2}\rho u^2 \tag{1}$$

where a is the vertical acceleration of the launch vehicle (for the ground experiment, $a = g$). Viscous force and surface tension can be neglected during the powered flight of launch vehicles. We assumed that all liquid drains through the toroidal control volume, indicated in Fig. 1 by a dotted-line area immediately before gas ingestion. This assumption is appropriate, because the dip grows rapidly, and the liquid velocity becomes large around the dip. Q can then be written as

$$Q = u\{2\pi R_b h_0 + 2\pi(R_b + \delta)h_0\} = 2u\pi h_0(2R_b + \delta) \tag{2}$$

Equations (1) and (2) give

$$h = h_0 + \frac{Q^2}{8\pi^2 a h_0^2 (2R_b + \delta)^2} \tag{3}$$

Gas ingestion to the feed line occurs immediately after the dip grows faster than the drop speed of the liquid level, or $\mathrm{d}h/\mathrm{d}h_0 = 0$; thus, h_c can be written as

$$\frac{h_c}{r} = \left[\frac{(r/R_b)^2 Fr}{8\{1 + (\delta/2R_b)\}^2}\right]^{1/3} \tag{4}$$

where

$$Fr = \frac{v^2}{2ra} \tag{5}$$

Fr, called the Froude number, is the ratio of the inertial to the gravitational forces.

Received 4 December 2009; revision received 27 May 2010; accepted for publication 2 June 2010.

*Engineer, Space Transportation Mission Directorate. Member AIAA.
†Senior Engineer, Space Transportation Mission Directorate.
‡Engineer, Engineering Digital Innovation Center. Member AIAA.
§Manager, Space System Department.
¶Engineer, Space System Department.

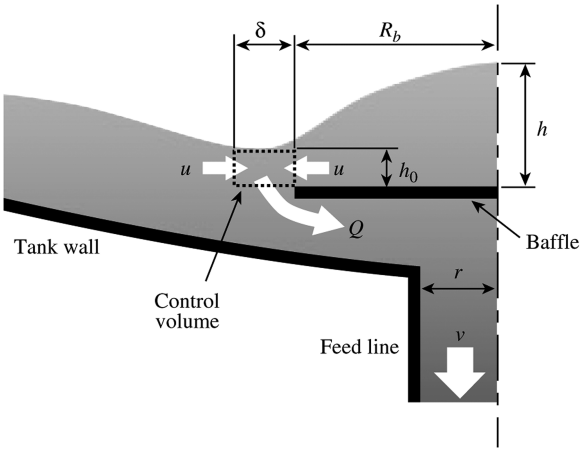

Fig. 1 Schematic of tank-draining problem.

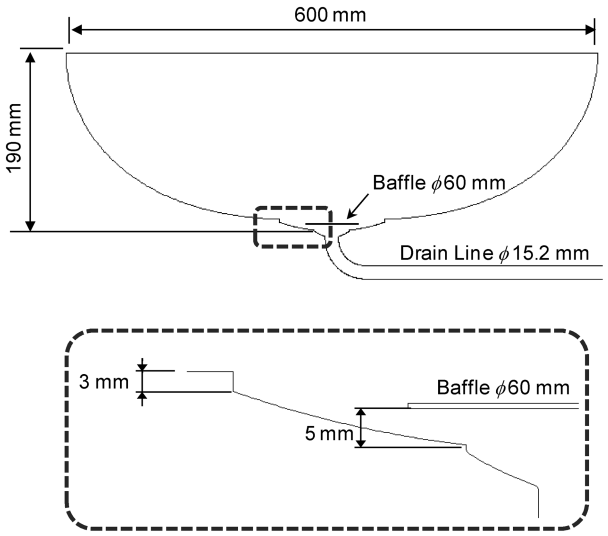

Fig. 2 Small-scale tank for draining experiment and close-up view of its outlet.

Equation (4) indicates that the Froude number and geometry around the tank outlet dominate the draining process. When the Froude number is identical and the outlet geometry is similar, the draining process is also similar, irrespective of the actual tank size. Therefore, by matching the Froude number and geometry, we can use a small-scale tank to predict the draining performance of a large-scale tank in an actual launch vehicle. When the Froude number is small, the gravitational force is greater than the inertial force, and the dip formation is restrained, because the surrounding liquids stream into the dip due to gravitational force, even if the dip is about to appear. In contrast, when the Froude number is large, dip formation is enhanced, and gas ingestion occurs.

Assuming that the dip appears near the baffle edge, or $2R_b \gg \delta$, Eq. (4) becomes

$$\frac{h_c}{r} = \left\{\frac{(r/R_b)^2 Fr}{8}\right\}^{1/3} \tag{6}$$

The situation is improved when R_b is large; however, the configuration for which this is true causes a large pressure drop through the baffle. The tradeoff must thus be carefully weighed for the design of the baffle.

III. Experimental Apparatus and Procedure

Experiments using full-scale tanks or real cryogenic inflammable propellants are clearly impractical. Therefore, we fabricated a small-scale tank for use in draining experiments to evaluate the liquid remaining at gas ingestion. The thermodynamic effects of the cryogenic propellants are significant for propellant management, although they hardly affect the draining process [9,10], and the Froude number is important from a fluid dynamics point of view. Hence, water was used as the draining fluid, because the Froude number is readily controlled by the water flow rate. Figure 2 shows the small-scale tank made of acrylic for easy observation of the water behavior. The inner diameter of the tank is 600 mm, which is at a scale of approximately one-fourth to one-eighth that of an actual launch vehicle. The drain line has a 90° elbow, and its radius r is 7.6 mm. The baffle design for the tank outlet requires the consideration of two factors: liquid remaining and pressure drop through the baffle. These requirements are contrasting and must therefore be determined uniquely for each launch vehicle. Our chosen geometry is also shown in Fig. 2, with a 3-mm-height step simulating a joint between the propellant-tank wall and a manhole.

Table 1 Froude numbers for different propellant types

Propellant	Froude number
LH_2	100–200
Liquefied natural gas	20–60
Kerosene	20–60
Liquid oxygen	20–60

Experiments were conducted under static and atmospheric conditions. The initial volume of water in the tank was 10,000 cc, corresponding to an 80 mm liquid level from the baffle surface; this is sufficient for minimizing the water-surface oscillation effects immediately before the gas ingestion. The drain flow rate was controlled using a valve and measured using a turbine flowmeter. Both were installed in the drain line. The time of gas ingestion was determined from a video recorded near the outlet and synchronized with the data logger. The volume flow rate at the start of the draining process was difficult to measure accurately; therefore, we installed a point-level sensor in the tank to determine when the water surface arrived at the fixed point that corresponds to the fixed water volume V_f. The liquid remaining V_r can be obtained by

$$V_r = V_f - \int Q \, \mathrm{d}t \tag{7}$$

The integral starts from when the water surface arrives at the fixed point through gas ingestion. The flow rate is almost constant during this interval. Therefore, any error in the start transition does not affect the liquid remaining. The shorter the integral interval, the higher the accuracy that we can obtain; this is because the flowmeter error accumulates with integral time. However, near the critical height, the water surface oscillates more, and the location of the fixed point becomes less certain. Considering these factors, the point-level sensor was set to approximately 3000 cc and carefully calibrated before every experiment.

The Froude number dominates the draining process. Typical Froude numbers during powered flight for several different propellant types are listed in Table 1. The Froude number for hydrogen is particularly large, because its low density leads to a high-flow velocity. Experiments were performed at 1 G, where the Froude number is controlled by the drain flow rate. We selected water flow rates of 300, 600, and 800 cc/s, corresponding to $Fr = 18.3$, 73.3, and 130.4, respectively; these values were chosen to approximately cover the range of values listed in Table 1.

IV. Numerical Methods

We developed a numerical simulation tool to describe the propellant-draining process. Both 2-D (axisymmetric) and 3-D simulations were conducted to evaluate the effect of draining asymmetricity due to the drain line elbow. The effect of turbulence was evaluated by conducting both turbulent and laminar flow

Table 2 Physical properties for calculation

	Water	Air
Density, kg/m^3	998.2	1.255
Viscosity, 10^{-5} kg/m/s	100.3	1.789
Surface tension, N/m	0.07274	——
Contact angle to the wall, °	75	——

calculations. Turbulent flow was simulated by the realizable k-ε turbulence model. The Navier–Stokes equation was spatially discretized by the finite-volume method, and the convective flux was evaluated by a second-order upwind scheme. Time integration was handled by a first-order-implicit noniterative time advancement algorithm. The air and water gas–liquid two-phase flow was modeled by the volume-of-fluid (VOF) method, and the surface tension of water was assumed to have a 75° contact angle to the wall. Values for the physical properties of water and air used are listed in Table 2. The liquid remaining in the tank was estimated in a similar manner to the experiments in which the front of the bubbles arrived at the drain line. Simulations started with 10,000 cc water in the tank, as in the case of the experiments.

The geometry used for the simulations was the same as that in the experiment (Fig. 2). The number of grids for the 2-D and 3-D simulations were 23,000 quadrilateral cells and 780,000 hexahedron cells, respectively. Only half of the domain was simulated for the 3-D cases, because the geometry was symmetrical. The cell distribution of the normal 2-D grid and radial cross section of the 3-D grid were similar; the minimum grid size was 0.125 mm around the baffle edge and the maximum was approximately 5 mm at the tank equator for both grids. The azimuthal interval was 5° for the 3-D grid, except near the center of the axis. For the boundary conditions, the atmospheric pressure was set at the tank equator, and flow discharged from the end of the drain line at the specified flow rate (300, 600, or 800 cc/s). The wall boundary condition was no slip.

We compared the VOF model with another simulation model based on the cubic-interpolated pseudo-particle-based level-set method (CIP-LSM) and some experiments in a previous study [11]. We confirmed that the models provided similar results for the surface behavior.

V. Experimental and Numerical Results and Discussions

A. Comparison of Liquid Remaining

Figure 3 shows a comparison of experimental, theoretical [calculated from Eq. (6)], and numerical simulation results for liquid remaining at gas ingestion. The theoretical critical height h_c was converted to liquid remaining at gas ingestion in order to compare the experimental and numerical results. The difference in liquid remaining at the critical height and gas ingestion is very small: that is, approximately 6 cc. The experimental error was estimated by replicating four times; it was approximately ±10% and was mainly caused by water-surface oscillation. The amplitude of oscillation, of the order of a few millimeters, depended on the flow rate. At 300 cc/s, the experimental and theoretical results were in good agreement. However, for 600 and 800 cc/s, the theoretical results underestimated the liquid remaining. The numerical simulation results revealed the reason for the same, as discussed next.

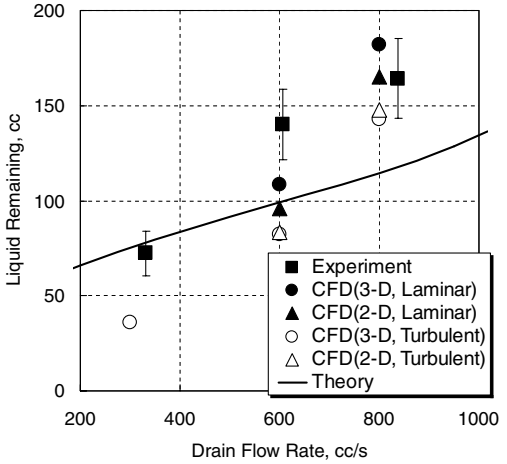

Fig. 3 Liquid remaining: comparison of experimental, theoretical, and numerical simulation results (CFD denotes computational fluid dynamics).

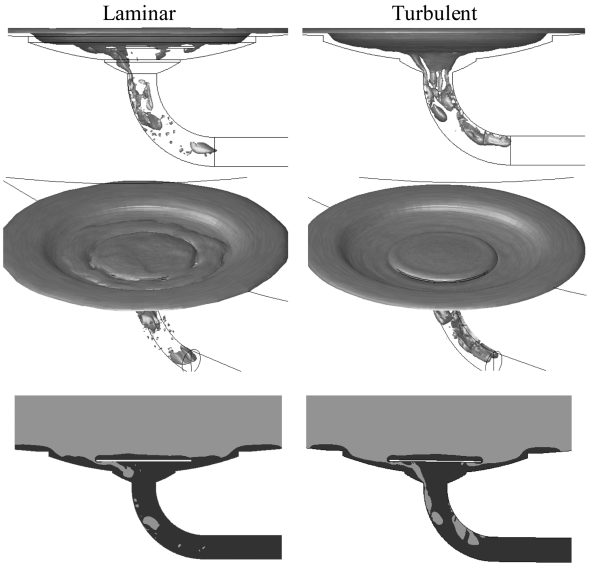

Fig. 4 Comparison of laminar and turbulent flow at gas ingestion (3-D, 600 cc/s).

B. Comparison of Laminar and Turbulent Flow

Figure 4 shows a comparison of laminar and turbulent flow results at gas ingestion for 3-D numerical calculations at a flow rate of 600 cc/s. The upper and middle parts of the figure show the isosurface for VOF = 0.5; the lower part of the figure shows the VOF distribution, or distribution of water and air. Although the turbulent flow was almost symmetric, the laminar flow became asymmetric. This is why the liquid remaining differed for the 2-D/laminar and 3-D/laminar cases (Fig. 3). The liquid remaining for the 2-D/turbulent and 3-D/turbulent cases was similar, because the turbulent flow was almost axisymmetric.

The bubble size was smaller for laminar flow than for turbulent flow, as shown in Fig. 4; this was because of the eddy viscosity of the turbulent flow, which prevented the generation of fine bubbles. The Reynolds numbers in the drain line (greater than 25,000) and around the baffle (greater than 30,000) were greater than the critical Reynolds number in the pipe flow (∼2000). Therefore, the flow regime could be turbulent around the baffle and in the drain line. The bubbles observed in the experiment flowed along the upper side of the drain line, as in the case of the turbulent flow simulation. With regard to the cell size, approximately 16 cells were required for proper bubble evaluation by VOF calculation [12]. The cell size was adequate for the turbulent flow.

However, the liquid remaining was closer to the experiment for laminar flow than for turbulent flow, as shown in Fig. 3. This was due to the water-surface oscillation, which increased the liquid remaining. Because the eddy viscosity in the turbulent flow reduced the surface oscillation, the oscillation in the laminar flow was larger than in the turbulent flow. The oscillation in the experiment, which was difficult to measure, was probably larger than in the simulations due to disturbances. Therefore, the order of liquid remaining was experiment to laminar to turbulent, as shown in Fig. 3; the vibration environment should be considered for accurate estimation of the liquid remaining in actual launch vehicles. To clarify draining processes around the outlet, such as dip formation and gas ingestion,

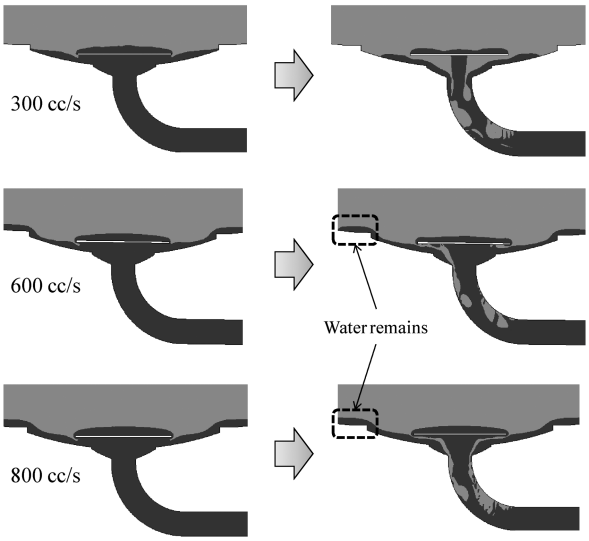

Fig. 5 Effect of flow rate on gas ingestion (3-D/turbulent).

applying the turbulent calculation is appropriate. Hence, the next discussions are based on the turbulent flow calculations.

C. Characteristics of Draining Flow

Figure 5 shows the effect of flow rate on gas ingestion for 3-D/turbulent calculations. Dip formation was almost symmetric in all flow rates. Water still remained on the horizontal flat surface above the step of the tank's inner wall at the moment of gas ingestion for 600 and 800 cc/s. The remaining volume on the step was approximately 31 cc for 600 cc/s and 75 cc for 800 cc/s, which is close to the difference between the experiment and theory (Fig. 3). The effect of the remaining liquid on the step was not considered in the theory presented in Sec. II; therefore, we can conclude that the theory properly describes draining without discontinuities of a tank's inner wall. However, the theory would be insufficient to evaluate the liquid remaining, and numerical simulation would be required if the tank inner wall had such discontinuities as most rocket tanks have. The water velocity in the tank was at a maximum at the surface of the dip near the baffle edge, in accordance with Bernoulli's law [Eq. (1)]; this is consistent with the theory presented in Sec. II.

D. Grid Sensitivity

To evaluate grid sensitivity, we conducted a finer-grid calculation for the 2-D/laminar drain flow rate at 600 cc/s. The finer-grid system had 92,000 cells, which is four times that of the normal grid system (23,000 cells). The resulting draining processes were confirmed to be similar. Thus, the normal grid system is sufficient for discussing the characteristics of the draining process. The resulting liquid remaining was 95.7 cc for the normal grid system and 117.2 cc for the finer grid system. The experimental result was 140.1 ± 18.3 cc, which is slightly closer to that of the finer grid system. A numerical accuracy study based on Richardson extrapolation [13] indicated that the fractional errors of the liquid remaining were roughly 19 and 1.2% for the normal- and finer-grid systems, respectively. The difference in liquid remaining was caused by the difference in water-surface oscillation. The finer-grid system exhibited larger oscillations because of its small numerical viscosity.

VI. Conclusions

Experiments and numerical simulations were performed to clarify the process by which liquid propellant drains from a small-scale tank in which the circular-plate-type device is near the outlet for application to future launch vehicle developments. Theoretical calculations based on Bernoulli's law indicate that Fr dominates the drain flow characteristics and appropriately describe draining without discontinuities of a tank's inner wall, which is helpful for preliminary design of the tank outlet. Experimental and simulation results for the liquid remaining are very similar; the slight differences between them are due to water-surface oscillation. Therefore, for the estimation of the liquid remaining in an actual launch vehicle, the vibration environment should be considered. The turbulent and laminar flow calculation results were proved to differ in their depiction of dip formation at the water surface and distribution of ingested bubbles; turbulent flow calculation was shown to be suitable for evaluating the flow around the tank outlet and the drain line based on experimental observations of the bubble behavior. In conclusion, VOF simulation considering flow turbulence is effective, even for actual propellants under most flight conditions ($Fr = 20$ to 130); we were able to show the potential effectiveness of the theory and we intend to apply the simulation to actual liquid-propellant draining under flight conditions in the future.

Acknowledgments

Experiments and simulations were performed with the cooperation of the experimental team of IHI Aerospace Company, Ltd., and Nobuaki Konishi of TGI Financial Solutions Company, Ltd. We express our gratitude to them.

References

[1] Norquist, L., "Development Progress, External Tank for the Space Shuttle Main Propulsion System," 14th AIAA/SAE Joint Propulsion Conference, AIAA Paper 1978-1004, 1978.

[2] Lacapere, J., and Vieille, B., "CFD Studies of Tank Draining: How to Enlarge the Qualification Field of ESC-A LOX Tank Anti-Vortex?" *International Astronautical Congress*, IAC-06-C4.3, Paris, 2006.

[3] Himeno, T., Watanabe, T., and Konno, A., "Numerical Analysis for Propellant Management in Liquid Rocket Tank," 37th AIAA/ASME/SME/SAE/ASEE Joint Propulsion Conference and Exhibit, AIAA Paper 2001-3822, 2001.

[4] Behruzi, P., and Dodd, C., "Future Propellant Management Device Concepts for Restartable Cryogenic Upper Stages," 43rd AIAA/ASME/SAE/ASEE Joint Propulsion Conference and Exhibit, AIAA Paper 2007-5498, 2007.

[5] Lubin, B. T., and Springer, G. S., "The Formation of a Dip on the Surface of a Liquid Draining from a Tank," *Journal of Fluid Mechanics*, Vol. 29, 1967, pp. 385–390. doi:10.1017/S0022112067000898

[6] Dodge, F. T., "Liquid Rotation and Vortexing During Draining," *The Dynamic Behavior of Liquids in Moving Containers*, NASA SP 106, 1966, pp. 373–377.

[7] Satterlee, H. M., and Hollister, M. P., "Low-G Propellant Tank Draining Problems," *Engineering Handbook Low-G Propellant Behavior*, NASA CR 92083, 1967.

[8] Berenyi, S. G., and Abdalla, K. L., "Vapor Ingestion Phenomenon in Hemispherically Bottomed Tanks in Normal Gravity and in Weightlessness," NASA TN D-5704, 1970.

[9] Greer, D., "Cryogenic Fuel Tank Draining Analysis Model," *Advances in Cryogenic Engineering*, Vol. 45, Part B, Kluwer Academic, Norwell, MA2000, pp. 1213–1220.

[10] Grayson, G. D., and Navickas, J., "Interaction Between Fluid-Dynamic and Thermodynamic Phenomena in a Cryogenic Upper Stage," AIAA 28th Thermophysics Conference, AIAA Paper 93-2753, 1993.

[11] Negishi, H., Himeno, T., and Yamanishi, N., "Numerical Analysis of Dynamic Behavior of Free-Surface Flows in Tanks Based on CIP-LSM," International Symposium on Space Technology and Science, ISTS Committee Paper 2006-a-04, Kanazawa, Japan, 2006.

[12] Sou, A., Hayashi, K., and Tomiyama, A., "A Volume Tracking Method for Multi-Phase Flow Simulation (Improvement of an Interface Reconstruction Method)," *Transactions of the Japan Society of Mechanical Engineers. Series B*, Vol. 70, No. 698, 2004, pp. 2538–2544 (in Japanese).

[13] Roache, P. J., "Perspective: A Method for Uniform Reporting of Grid Refinement Studies," *Journal of Fluids Engineering*, Vol. 116, No. 3, 1994, pp. 405–413. doi:10.1115/1.2910291

T. Lin
Associate Editor